Scientia Iranica A (2019) 26(6), 3072–3084

SCIENTIA IRANICA

Sharif University of Technology
Scientia Iranica
Transactions A: Civil Engineering
http://scientiairanica.sharif.edu

Effect of FRP strengthening on the SHS brace collapse mechanism

P. Shadan and M.Z. Kabir*

Department of Civil Engineering, Amirkabir University of Technology, 424 Hafez Avenue, Tehran, Iran.

Received 5 June 2016; received in revised form 8 November 2017; accepted 7 July 2018

KEYWORDS
Stability;
Strengthening;
CFRP;
Square hollow section brace;
Numerical study.

Abstract. During an earthquake, diagonal braces are designed to dissipate energy by yielding in tension and buckling in compression. However, local buckling occurring in the middle of the brace leads to immediate fracture. Aiming to strengthen braces against local buckling, this study proposes wrapping FRP sheets in the transverse direction. The effect of FRP strengthening on the post-buckling behavior of Square Hollow Section (SHS) tubes has not been investigated. A numerical model was generated and verified by other previous researches. Then, a comprehensive parametric study was conducted, and the effects of slenderness ratio, the number of FRP layers, and FRP coverage percentage on post-buckling response of the strengthened brace were explored within this study. Results indicated that utilizing FRP was certainly successful in mitigating local buckling mode of long SHS braces. Moreover, for short braces, applying enough FRP layers can change the mode of buckling from local to overall. Finally, an optimized length of FRP was proposed for brace strengthening in accordance with their slenderness ratio.

1. Introduction

Due to their numerous advantages, SHS section is used extensively as a bracing member. During an earthquake, a diagonal brace member undergoes several tension-compression cycles. Yielding in tension, buckling in compression, and a plastic hinge formation at the mid-span help a brace to dissipate ground motion energy. However, by accumulating plastic deformation, local buckling develops within the plastic hinges, leading to failure after a number of cycles [1-3]. Thus, with a more belated local buckling formation, a brace can have a more energy dissipation capacity. However, the local buckling threat to SHS tubes as a thin-walled section is inevitable [4,5]. Limitations on the compactness ratio were assigned to seismic provisions as a remedy to inhibit the local buckling mode [6,7]. Despite the fact that decreasing the compactness ratio is a practical way to prevent local buckling, it may lead to an increase in weight and cost. In addition, some researchers investigated and recommend using innovative sections with higher resistance against local buckling [8,9]. However, the deficiency of compactness should still be compensated for numerous existing buildings.

Welding steel plates to steel structures is another way for strengthening steel structures against local buckling. However, it is not desirable due to an increase in weight and residual stresses caused by welding. Fibre-Reinforced Polymer (FRP) composites have been recently used as a strengthening component. As acknowledged by previous researches, FRP can be used as a promising approach to concrete structures [10-12]. However, the beneficial effects of FRP strengthening on steel structures are still under investigation [13,14]. High strength-to-weight ratio, good corrosion resistance, and absolute shape flexibility of FRP are the

*. *Corresponding author. Tel.: +98 21 64543000; Fax: +98 21 66414213*
E-mail address: mzkabir@aut.ac.ir (M.Z. Kabir)

doi: 10.24200/sci.2018.20690

most noticeable advantages of FRP that encourage the construction industry to use it as a strengthening material. It can not only enhance the flexural behavior of structural elements [15-17], but also strengthen the stability of steel members, as recently discovered.

Some researchers [18-20] investigated the effects of Carbon Fibre-Reinforced Polymer (CFRP) and Glass Fibre-Reinforced Polymer (GFRP) wrapping on the plastic hinge performance. They demonstrated that CFRP could expand the plastic hinge zone, delay the lateral torsional buckling, and slow down the local buckling occurrence. Sayed-Ahmed [21] added CFRP layers to non-compact tension flange of the I-shape sections to increase flexural strength by delaying the local buckling incident. Moreover, it was shown that the threat of buckling could be avoided by FRP enhancement for slender structures without a significant gain in weight [22,23].

FRP composites were also used for increasing the axial capacity of columns. Shaat and Fam [24-26] applied FRP laminates to long columns and investigated the effect of longitudinal FRP sheets on the global buckling load of columns for different slenderness ratios. They also utilized FRP sheets on short columns in both transverse and longitudinal directions to inspect the effect of FRP direction on the local buckling strength. According to the results obtained, for long columns, the effect of strengthening was decreased by reducing slenderness ratio; for short columns, transverse layers were more effective in mitigating local buckling. The effect of CFRP strengthening on column behavior was also examined, and the obtained results indicated that CFRP wrapping could be reliably used for enhancing axial compression strength of columns [27-30]. Kabir and Nazari [31] studied the buckling of cracked tubes repaired by FRP. They found that the application of FRP patch could retrieve the whole strength of the damaged tube; in some cases, it could even enhance the strength by 35% in comparison with the intact column. Furthermore, in order to reduce the local buckling effects on circular steel tubes, researchers [20,32-34] demonstrated that utilizing FRP wrapping could be an efficient solution. Moreover, Zhao et al. [35] confirmed that CFRP bonding could increase the end-bearing capacity of the RHS tubes. Alam et al. [36] demonstrated the success of FRP wrapping in enhancing the impact-resistance capacity of steel tubular members. Moreover, some researchers demonstrated the success of FRP wrapping in confining concrete-filled steel tubes [29,37,38].

Some studies investigated FRP strengthening of braces. Harries et al. [39,40] added FRP plates to T section flanges to prevent local buckling in web and flange. They realized that FRP could control local buckling formation before debonding, while the effect of FRP was reduced by increasing the slenderness ratio. Gao et al. [41] strengthened long tube braces with CFRP in the longitudinal direction to increase the overall buckling. They concluded that longitudinally bonded CFRP sheets were really effective in increasing axial strength. El-Tawil and Ekiz [42] inhibited brace buckling by wrapping FRP sheets to provide a similar response of Buckling-Restrained Braces (BRB).

Although previous studies have shown that FRP composites could enhance the performance of the structural members subject to buckling phenomenon, the FRP strengthening of braces with square hollow sections against local buckling has not been investigated so far. Accordingly, this study evaluated the effect of transverse wrapped CFRP on buckling modes of the SHS braces. To do so, numerical models for the brace strengthening were developed by ABAQUS (2011), while the effects of various parameters, including slenderness ratio, number of FRP layers, and FRP coverage length, were investigated.

2. Finite-element modeling of CFRP strengthened SHS braces

To provide a ductile response in an earthquake scenario, diagonal braces must be designed to sustain plastic deformations and dissipate hysteretic energy in a stable manner through successive cycles of buckling in compression and yielding in tension [43]. Therefore, the brace strengthening should be performed such that it has no effect on the overall buckling, since the brace needs to buckle in compression to dissipate earthquake energy. Instead, CFRP should be able to reinforce the brace against local buckling, which causes rupture. In comparison to the achievements of previous investigations, in this research, the effect of FRP application in the transverse direction was studied in a wide range of SHS braces. Thus, the effect of strengthening on the post-buckling behavior of the braces, which has not been considered by other studies, was explored.

In order to investigate the performance of CFRP strengthened SHS braces, a finite element study was conducted by using ABAQUS. As illustrated in Figure 1, the model is composed of an SHS brace and

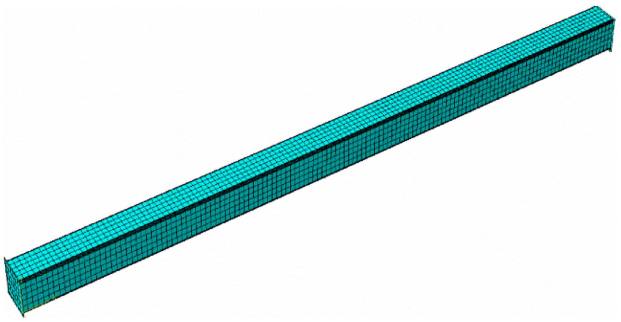

Figure 1. A typical view of the model developed by ABAQUS.

FRP sheets, which were wrapped transversely around the entire length of the brace. The cross-section used in the numerical study was the same with that in the experimental tests reported in Shaat [24]. It was an $89 \times 89 \times 3.2$ mm SHS, which is a non-compact section in accordance with AISC [7]. Therefore, the section is prone to local buckling incident. Both FRP sheets and steel section were modeled with shell elements, which are suitable for large-scale deformation analysis.

2.1. Material model

All the material properties were extracted from Shaat study [24], as listed in Table 1. The bilinear isotropic hardening model was considered for steel behavior, and the tangent modulus was assumed to be 0.5% of elastic modulus. Buckling behavior of cold-formed steel members was affected by residual stresses, which were considered by inserting residual stress pattern, displayed in Figure 2, into the Gauss points, too [44,45]. In this figure, t shows the thickness of the section. Hashin criterion was chosen for evaluating the FRP composites failure [46]. The Hashin failure criterion is appropriate for orthotropic material with brittle behavior, and the criterion viably used for the failure prediction of FRP composite materials was confirmed by previous studies [47,48]. The bond between tube and FRP was also modeled by employing the cohesive behavior option [46]. The required inputs were calculated through the equations shown in [49]. However, debonding was not checked and bond simulation was done to consider the effect of bond strength loss on the buckling incident.

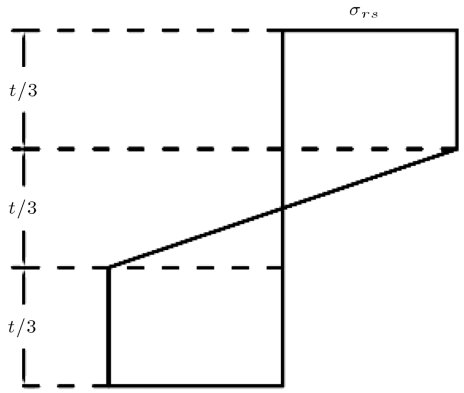

Figure 2. Residual stress pattern [44].

2.2. Loading and boundary conditions

To simulate boundary conditions closer to the real-world practice, base plates were also included in the modeling and the axial load was exerted on the brace through them. In braced frames due to the plastic hinge formation in gusset plate connection, the brace member is in the situation of hinged-hinged boundary condition. Thus, the rotation degree of freedom at both ends was released.

Two loading conditions of monotonic and cyclic loading were investigated. For monotonic analysis, models were axially compressed till local buckling in the braces was formed. For cyclic analysis, modified Applied Technology Council (ATC) loading protocol, recommended by Fell [2] for concentric braces, was selected. Figure 3 shows the modified ATC loading protocol. In this figure, drift angle (θ) is the rotation of braced frame, and the corresponding axial displacement (Δ_a) can be calculated by Eq. (1):

$$\Delta_a = 0.5 L_B \theta, \tag{1}$$

where L_B is the length of the brace.

2.3. Validation of the model

Since the model should be able to capture both local and global buckling modes, six columns with lengths of 2380 mm and 175 mm dominating global and local buckling modes, respectively, were selected from Shaat's study [24] and modeled. First, control specimens from both long and short columns, called 7 and 12, were verified. Then, two long columns, including that on two sides of the section (named 8) and the

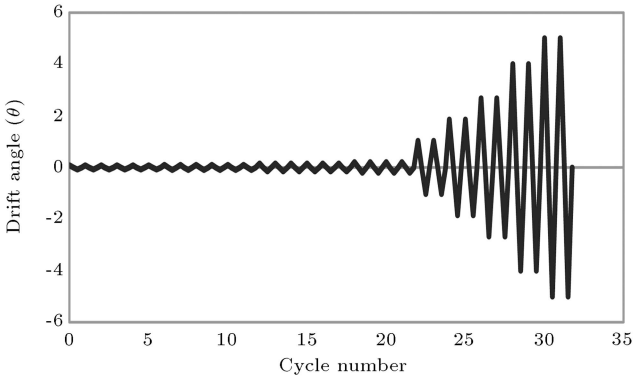

Figure 3. Cyclic loading history [2].

Table 1. Material properties.

Material	Yield strength (MPa)	Tensile strength (MPa)	Tensile modulus (GPa)	Rupture strain (%)
Steel	382	-	200	-
CFRP	-	1132	114	1
GFRP	-	336	17.6	2
TYFO S	-	72.4	3.18	5

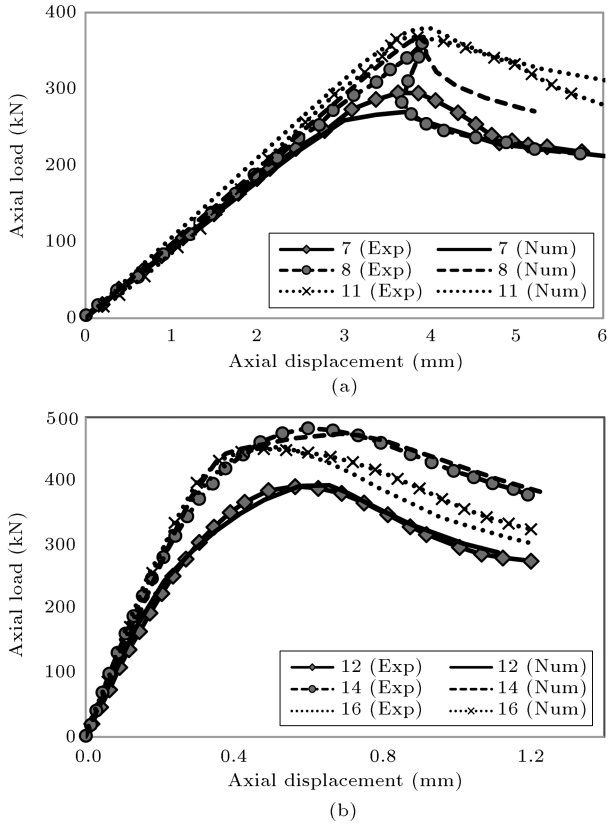

Figure 4. Validation of a numerical model with experimental results reported in [24]: (a) Long column ($kL/r = 68$) and (b) short column ($kL/r = 4$).

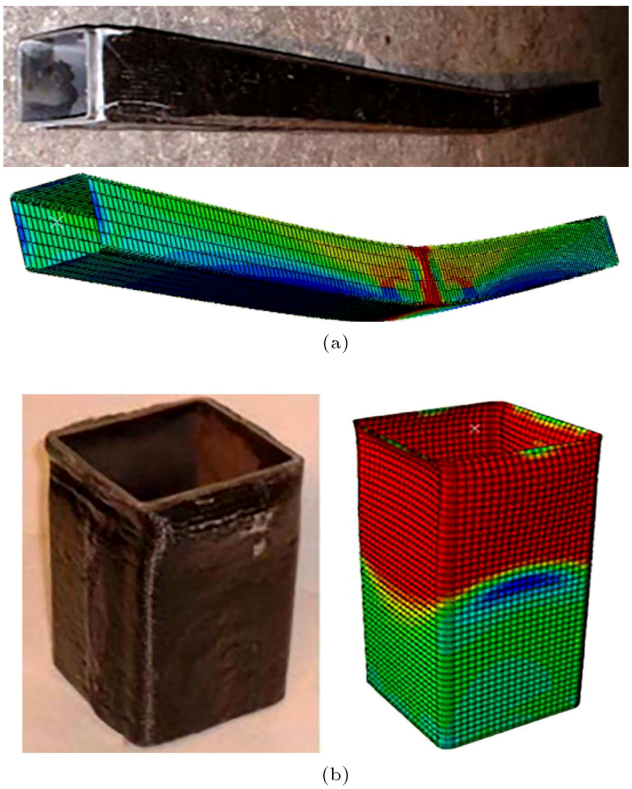

Figure 5. Validation of the buckled shape obtained from numerical model with those given by experimental tests reported in [24]: (a) Long brace with a slenderness ratio of 68 and (b) short brace with a slenderness ratio of 4.

other on all four sides (named 11), strengthened with longitudinal CFRP were verified, too. Specimen 14 was strengthened with wrapping FRP sheets in the transverse direction, and Specimen 16 was strengthened by wrapping both longitudinal and transverse layers of CFRP. As expected, after buckling, the strength of columns gradually dropped. According to Figure 4, the numerical model can accurately be validated against experimental results [24] for both unstrengthened and strengthened specimens. The developed numerical model also has a good ability to capture the buckled shape (see Figure 5).

3. Effect of FRP wrapping on buckling behavior

As mentioned in the previous sections, the local buckling is not a desirable failure mode for braces under cyclic loading. Therefore, the strengthening should merely enhance the performance of the member under local buckling with no effect on the global buckling, since the overall buckling will enable the brace to dissipate earthquake energy. According to previous studies [24], utilizing FRP in the transverse direction can inhibit local buckling by controlling outward buckling of two sides (see Figure 6).

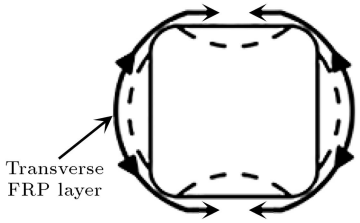

Figure 6. Effect of transverse FRP layer on local buckling [24].

In the current research work, a layer of GFRP and two layers of CFRP were transversely overwrapped through the entire length of the brace, and their effect on the local buckling was investigated for different slenderness ratios.

3.1. Eigenvalue analysis of braces with different slenderness ratios

The elastic buckling (eigenvalue) analysis was carried out to find the buckling mode shapes of the braces. However, since the response of the braces involves material nonlinearity, a general eigenvalue buckling analysis can only provide a useful understanding of buckling mode shapes. In addition, geometry imperfections used for post-buckling analysis are generated from the lowest buckling mode shapes [46]. While shorter braces buckle

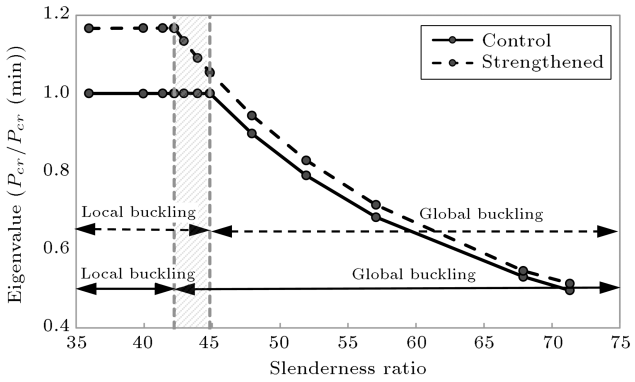

Figure 7. The normalized values of elastic buckling load with respect to the slenderness ratio.

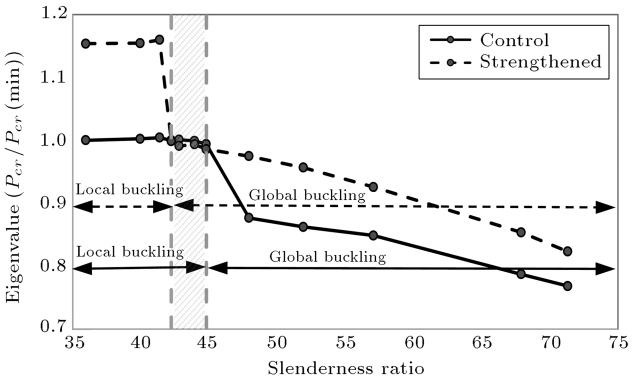

Figure 8. Critical buckling load versus slenderness ratio developed by post-buckling analysis.

locally, the buckling mode changes from local to global when slenderness ratio is more than 44.8, as shown in Figure 7. The vertical axis of Figure 7 indicates critical elastic buckling load (P_{cr}) normalized against a critical elastic buckling load of the shortest control model (P_{cr} (min)), while the horizontal axis shows the slenderness ratio. It is seen that when the brace is strengthened by CFRP, the slenderness ratio, the border between two buckling modes, is reduced to 42.2.

The slenderness ratio range of both control and strengthened models was divided into two parts of the local and global buckling regions. As can be seen, there is a middle part, where the dominant mode of control braces is still local buckling, whereas the strengthened braces buckle globally. This middle part is marked with hatch patterns in the figure. This reveals that FRP-strengthening can transform the mode of buckling from local to global for the specific slenderness ratio range. For convenience, the part where both strengthened and unstrengthened braces begin to buckle locally is called short brace part. The part where only unstrengthened braces have local buckling mode is called intermediate brace part, and wherever the global buckling dominates is called long brace part.

3.2. Post-buckling analysis of braces with different slenderness ratios

A nonlinear static analysis using modified Riks method was also conducted to explore the effect of strengthening on the buckling behavior of braces considering material nonlinearities. Thus, the ultimate strength of braces (P_{cr}) with different slenderness ratios was computed. Results are illustrated in Figure 8. The vertical axis shows the ultimate strength of the braces (P_{cr}). The axis is normalized against the minimum ultimate strength ($P_{cr(\min)}$), which belongs to the shortest control brace. The borders between local and global buckling were found the same as those obtained from eigenvalue analysis. By considering plastic behavior during the analysis, the difference between buckling loads of control and strengthened models narrows down, compared to the results of eigenvalue analysis. While the local buckling mode of short braces is length independent, their critical buckling load does not change with the slenderness ratio growth. However, when the global buckling mode is dominant, the critical buckling load of the braces decreases by increasing the slenderness ratio. According to Figure 8, for the short brace part, strengthening has the highest role in increasing the buckling strength. However, for intermediate brace part, by providing a sufficient compactness ratio, strengthening transferred local buckling to the second position, which caused brace to buckle globally with lower strength.

In the long brace part, the effect of strengthening on critical buckling load diminishes gradually, which indicates the limited efficiency of strengthening in the overall buckling.

Figure 9 shows the axial load-axial displacement diagrams for both short and long braces. As depicted in this figure, only local buckling takes place at the ends for short braces, although local buckling following global buckling appears in the middle of the brace for long braces. The variations in the load reduction rate of the diagram, caused by buckling modes, are shown in Figure 9(b).

Because the local buckling point of long braces is located in the descending part of the axial load-axial displacement graph, investigating the effect of strengthening may not be applicable. Hence, there is a need to define a parameter that can infer local buckling mitigation properly.

The axial displacement is the only parameter that increases linearly with respect to time. Therefore, by considering the axial displacement accompanied by the occurrence of local buckling as δ_{LB}, parameter $\Delta\delta_{LB}$ was defined for evaluating the local buckling enhancement. $\Delta\delta_{LB}$ can be calculated using Eq. (2).

$$\Delta\delta_{LB} = \frac{\delta_{LB_{\text{Strengthened}}} - \delta_{LB_{\text{Control}}}}{\delta_{LB_{\text{Control}}}} \times 100\%. \qquad (2)$$

Hence, a greater amount of $\Delta\delta_{LB}$ shows more delay

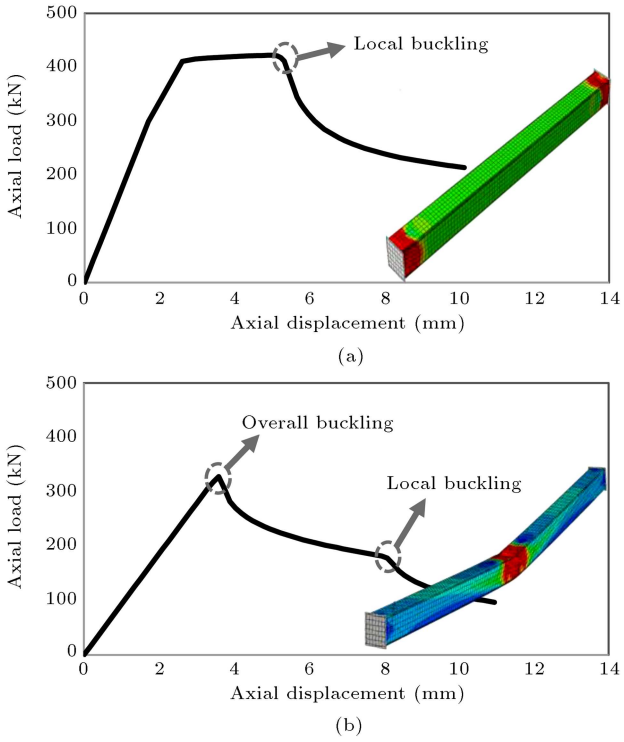

Figure 9. Axial load-axial displacement response for short and long braces: (a) Buckling modes of short brace and (b) buckling modes for long brace.

in local buckling incident. Details of the obtained results are listed in Table 2. P_y, in this table, is the load through which steel starts to yield; P_{cr} is the ultimate load that a specimen can tolerate. Under load P_u, fracture initiates and δ_u is the corresponding displacement of load P_u. Another parameter, $\Delta\delta_u$, was also defined that expressed an improvement in postponing the fracture initiation.

After strengthening, the amount of P_{cr} increased reasonably for short braces. However, the amount of P_{cr} for long braces did not undergo notable change. For intermediate braces with slenderness ratios between 42.2 and 44.8, mode transformation, which is caused by strengthening, decreased the ultimate strength, P_{cr}. Besides, strengthening did not make a notable change in P_y parameter. The growth of $\Delta\delta_{LB}$ in long braces shows that strengthening is remarkably successful in delaying local buckling incident.

The amplified amount of $(\Delta\delta_{LB})$ for slenderness ratios between 42.2 and 47.9 corresponds to the change in buckling mode sequence caused by strengthening.

The way that all of these parameters are altered proves that strengthening in the transverse direction is effective in postponing local buckling with no considerable rise in global buckling load, as expected. In addition, an insignificant increase in P_y indicates that the strengthening strategy does not even block the plastic flow in the section, which is helpful for earthquake energy damping. Moreover, a large amount of $\Delta\delta_u$ parameter for moderate and long models reveals that by delaying the local buckling formation, the occurrence of fracture can be inhibited essentially. For short models, this parameter has lower growth. The reason is that strengthening short braces increases their strength capacity against local buckling, while postponing it as the local buckling is the dominant mode for them. The last column of the table shows the observed failure modes. Y, GB, LBE, LBM, and DB represent Frac mean yielding, global buckling, local buckling at the end of the brace, local buckling in the middle of the brace, debonding and fracture, respectively. The failure of all cases resulted in a fracture, caused by local buckling development.

4. Effect of FRP wrapping on cyclic response

During an earthquake, brace members are exposed to cycles of tension and compression. Then, the effect of FRP strengthening on the brace hysteretic performance should be clarified, too. For this reason, the cyclic response of a wide range of unstrengthened and strengthened braces with different slenderness ratios was investigated.

As a sample, the axial cyclic response of a long strengthened brace, obtained from numerical analysis, is compared to the control one, as presented in Figure 10. In this figure, axial load is normalized against plastic load, and axial displacement is normalized against plastic displacement. It is noticeable that strengthening by inhibiting local buckling in compressive part is able to postpone the brace strength loss occurrence in tensile part of the next cycle. In addition, strengthening brought about a wider diagram, which proves the efficiency of strengthening in cyclic performance enhancement.

Two fundamental factors in evaluating the brace hysteretic performance include ductility and energy

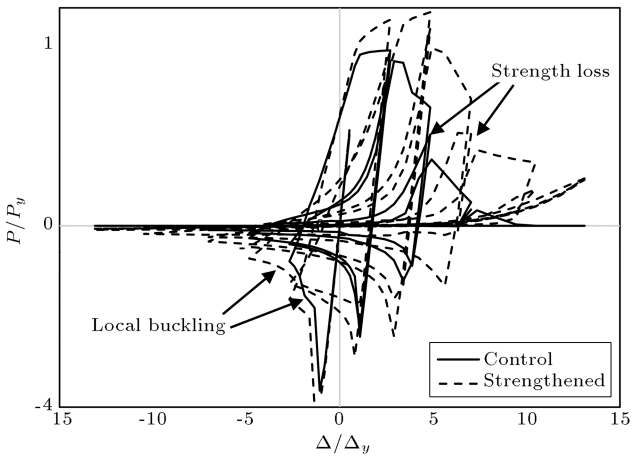

Figure 10. Comparing the hysteretic response of control and strengthened braces.

Table 2. Effect of slenderness ratio on strengthening of brace.

λ	P_y (kN)	P_{GB} (kN)	P_{LB} (kN)	δ_{LB} (mm)	P_{cr} (kN)	δ_{cr} (mm)	P_n (kN)	δ_u (mm)	ΔP_y (%)	ΔP_{cr} (%)	$\Delta\delta_{LB}$ (%)	$\Delta\delta_u$ (%)	Mode of fail.
35.9	411	-	418	3.3	422	4.9	368.7	5.6	-	-	-	-	Y-LBE-Frac
39.9	390	-	418	3.49	422	5.5	365.2	5.9	-	-	-	-	Y-LBE-Frac
41.4	386	-	418	3.66	422	5.7	363.5	5.9	-	-	-	-	Y-LBE-Frac
42.2	378	-	417	3.75	422	5.6	362.4	6.2	-	-	-	-	Y-LBE-Frac
42.8	374	-	417	3.88	422	5.8	360.1	6.3	-	-	-	-	Y-LBE-Frac
43.9	361	-	416	3.92	420	5.9	359.8	6.7	-	-	-	-	Y-LBE-Frac
44.8	355	-	414	3.98	421	6	358.6	6.8	-	-	-	-	Y-LBE-Frac
47.9	340	365	263	5.02	365	2.9	195.4	5.8	-	-	-	-	Y-GB-LBM-Frac
51.9	316	359	238	5.86	359	3.1	186.9	6.3	-	-	-	-	Y-GB-LBM-Frac
57	326	353	222	6.2	353	3.3	175.8	6.6	-	-	-	-	Y-GB-LBM-Frac
67.9	318	328	178	8.1	328	3.6	139.9	8.7	-	-	-	-	Y-GB-LBM-Frac
71.3	314	320	175	8.15	320	3.7	138.9	8.9	-	-	-	-	Y-GB-LBM-Frac
						Strengthened							
35.9	436	-	481	4.6	484	5.4	376	6.5	6.2	14.7	39.4	16.1	Y-LBE-Deb-Frac
39.9	411	-	481	5.7	485	6.1	371	7.1	5.3	15.0	63.3	20.3	Y-LBE-Deb-Frac
41.4	397	-	483	6	487	6.4	370	7.2	3.0	15.5	64	22	Y-LBE-Deb-Frac
42.2	390	416	306	8.9	416	2.8	212	10.5	3.1	–1.3	143	69.3	Y-GB-LBM-Deb-Frac
42.8	387	413	208	9.8	413	3	200	10.8	3.5	–2.1	152	69.0	Y-GB-LBM-Deb-Frac
43.9	379	414	265	9.9	414	3	192	11.4	5.1	–1.6	152	70.1	Y-GB-LBM-Deb-Frac
44.8	372	411	279	9.95	411	3	196	11.5	4.9	–2.5	150	69.1	Y-GB-LBM-Deb-Frac
47.9	369	406	256	10.5	406	3.1	183	11.8	8.4	11.2	109	103	Y-GB-LBM-Deb-Frac
51.9	344	398	218	11.4	398	3.3	165	12.9	8.7	10.9	94.5	104	Y-GB-LBM-Deb-Frac
57	342	386	219	11.7	386	3.4	159	13.7	9.3	9.2	89.2	107	Y-GB-LBM-Deb-Frac
67.9	335	356	167	15.3	356	3.7	109	21.4	9.48	8.5	88.8	145	Y-GB-LBM-Deb-Frac
71.3	332	343	159	15.4	343	3.8	101.1	24.9	9.6	7.11	88.9	179	Y-GB-LBM-Deb-Frac

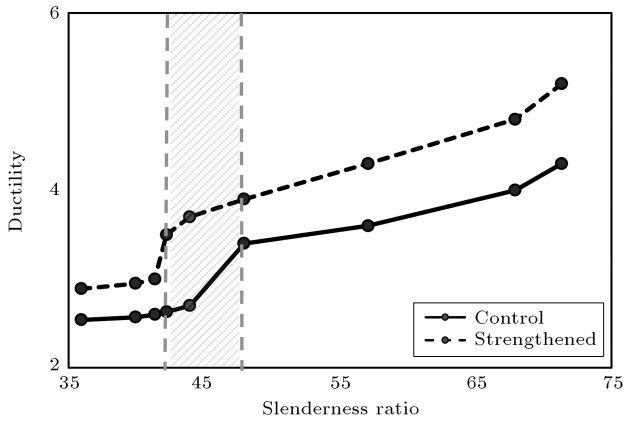

Figure 11. Ductility versus slenderness ratio developed by cyclic analysis.

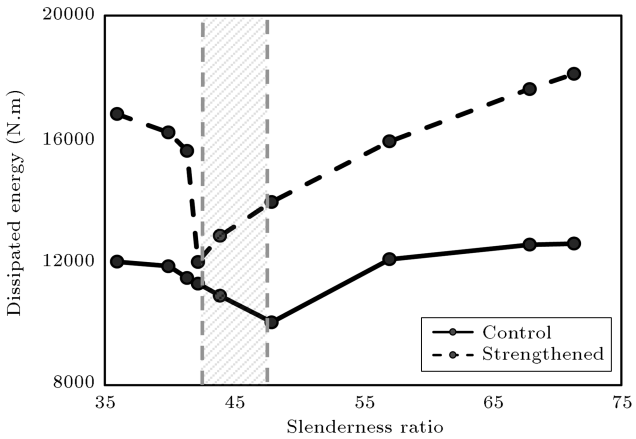

Figure 12. Dissipated energy versus slenderness ratio developed by cyclic analysis.

dissipation. These two factors were computed for both strengthened and control models, and the results are illustrated against the slenderness ratio in Figures 11 and 12.

In accordance with the figures, seismic demands increased with the slenderness ratio growth for long braces, whereas no significant variation was seen for short braces. This corresponds to the later local buckling incident of longer braces, leading to later failure. In addition, FRP strengthening led to an increase in ductility and energy dissipation capacities of braces in all of the three parts. This is not surprising, while FRP wrapping in the transverse direction did not

prevent yielding or overall buckling incidents, which are the prerequisites for ductile behavior.

5. Parametric study of the strengthening characteristics

A parametric study was carried out by the developed finite element model to optimize CFRP utilization. Thus, a brace from each category of short, intermediate, and long braces was selected, and the effects of two strengthening parameters, including coverage length and the number of FRP layers, were investigated.

5.1. Effect of FRP coverage length

Since the local buckling is prone to occur in specific locations, strengthening the entire length of brace does not seem to be necessary. Hence, in this section, the effect of FRP coverage length on the local buckling is reported. Then, 25%, 50%, 75%, and 100% of the brace length were covered by CFRP, and the axial response of the braces as well as their buckling mode shapes were investigated. The strengthening layup was considered to be the same as before.

5.1.1. Short braces

A short brace with a slenderness ratio of 35.9 was selected. As shown in Figure 9(a), local buckling for short braces forms at two ends of the brace. Thus, for the purposes of partial strengthening, only the end parts were equally covered, as shown in Figure 13.

Figure 14(a) displays the influence of partial strengthening on axial load-axial displacement relationships of the short brace. It is observed that, due to the dependency of the local buckling on the compactness ratio, partial strengthening may not postpone the local buckling. In other words, by strengthening the end parts, the local buckling was just transferred from ends to the middle with no improvement in buckling strength (see Figure 14(b)). However, when the entire length of the brace was covered with CFRP, the buckling load increased remarkably. Consequently, partial strengthening is not effective in the case of short braces.

5.1.2. Intermediate braces

An SHS brace with a slenderness ratio of 42.8 was also selected from the intermediate brace category. Since the buckling mode of unstrengthened intermediate

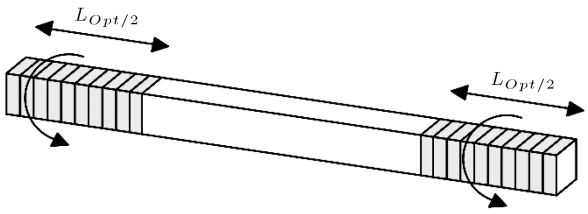

Figure 13. Strengthening strategies for short and intermediate braces.

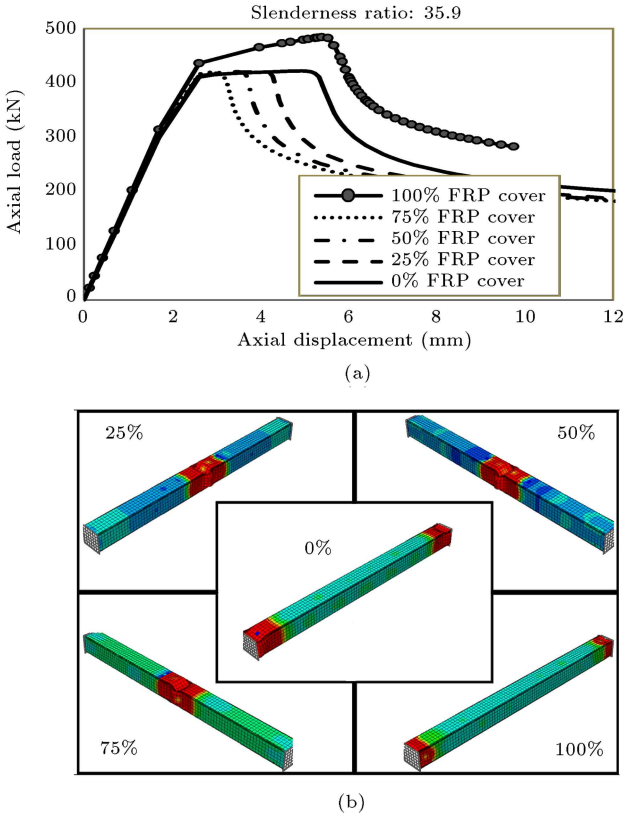

Figure 14. Effect of partial strengthening on the buckling behavior of the short brace: (a) Axial load-axial displacement relationship and (b) buckling mode shape.

braces is similar to that of short braces, a similar strengthening pattern was used (see Figure 13). In the previous sections, it was shown that strengthening the entire length could change the buckling mode of the intermediate brace from local to global buckling. However, as shown in Figure 15, with the partial strengthening, local buckling mode governed the behavior of the strengthened brace. Moreover, according to Figure 15(a), partial strengthening cannot improve the buckling strength of the brace, too. Thus, partial strengthening is not a practical technique for intermediate braces. By full strengthening (100% in Figure 15), as expected, the buckling mode of the brace changed; however, no increase was observed in the buckling load of the brace.

5.1.3. Long braces

Among long braces, a brace with a slenderness ratio of 67.9 was chosen. The local buckling for long braces occurs after global buckling in the middle of the brace. Therefore, the middle part needs to be strengthened (see Figure 16).

The results of partial strengthening of long braces are illustrated in Figure 17. As depicted in Figure 17(a), while the coverage length does not have an effect on the global buckling which controls the

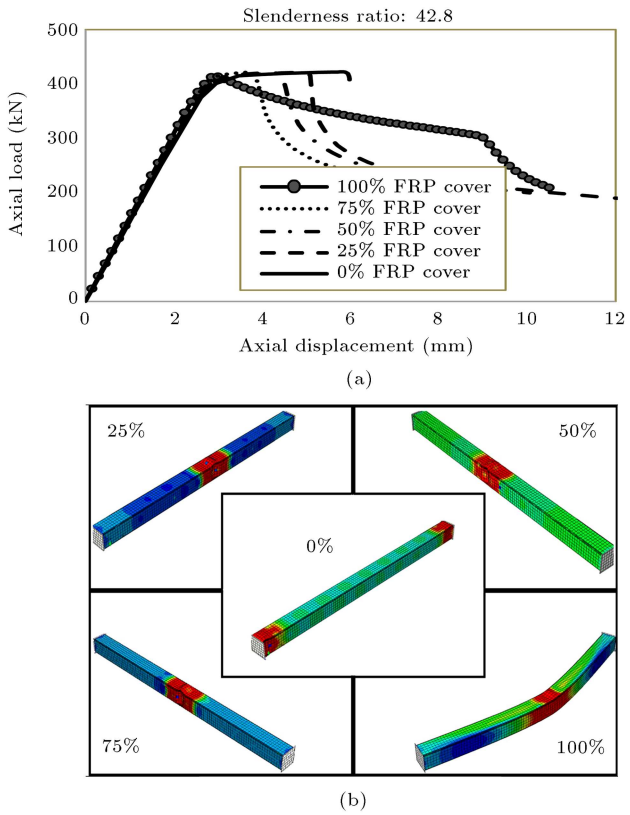

Figure 15. Effect of partial strengthening on buckling behavior of the intermediate brace: (a) Axial load-axial displacement relationship and (b) buckling mode shape.

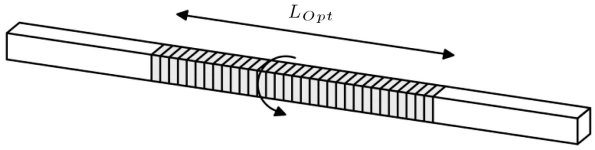

Figure 16. Strengthening strategies for the long brace.

strength of the brace, it significantly postpones the local buckling. In addition, decreasing the coverage length does not reduce the effectiveness of retrofitting in local buckling mitigation. However, as shown in Figure 17(b), when the FRP strengthened region is not long enough, the local buckling forms outside of strengthened region close to the ends of strengthening region. Therefore, in order to conduct effective partial strengthening, FRP coverage length should be long enough to inhibit all the local buckling possibilities inside and outside of the strengthened region. For a brace with a slenderness ratio of 67.9 and compactness of 24.8, strengthening at least 50% of the brace length is recommended.

Since slenderness and compactness ratios have key roles in the behavior of long braces, the effect of these two parameters on the optimum length of FRP coverage length was studied, too. The optimized length of FRP coverage of a brace with an $89 \times 89 \times 3.2$ mm

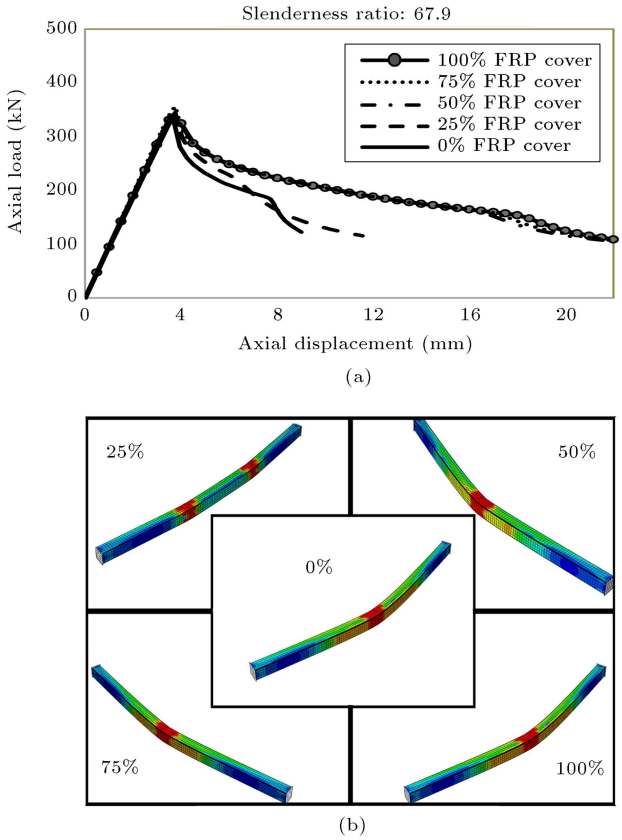

Figure 17. Effect of partial strengthening on the buckling behavior of the long brace: (a) Axial load-axial displacement relationship and (b) buckling mode shape.

section was determined for different slenderness ratios. Results are illustrated in Figure 18(a). According to the figure, by increasing the brace's slenderness ratio, the required length of FRP decreased. Furthermore, the optimized percentage of FRP coverage was converged to about 40% for the slenderness ratios, i.e., more than 86.

A similar study was performed on the compactness ratio. The variations of the optimized FRP coverage length with a compactness ratio are given in Figure 18(b) for a brace with a slenderness ratio of 67.9. When the compactness ratio increased to 37, the entire length of the brace was required to be strengthened as the local buckling dominated. However, for a less compactness ratio, the optimized FRP coverage length varied between 65% and 33%. With a reduction in compactness ratio, the optimized length of FRP coverage decreased.

5.2. Effect of the number of FRP layers

In this section, the number of FRP layers required for providing adequate compactness is explored. The braces selected in the previous sections are used for this section, too. To do so, a layer of GFRP was considered to be glued as the first layer for all braces, while the number of CFRP layers varied from 1 to 4. Of note,

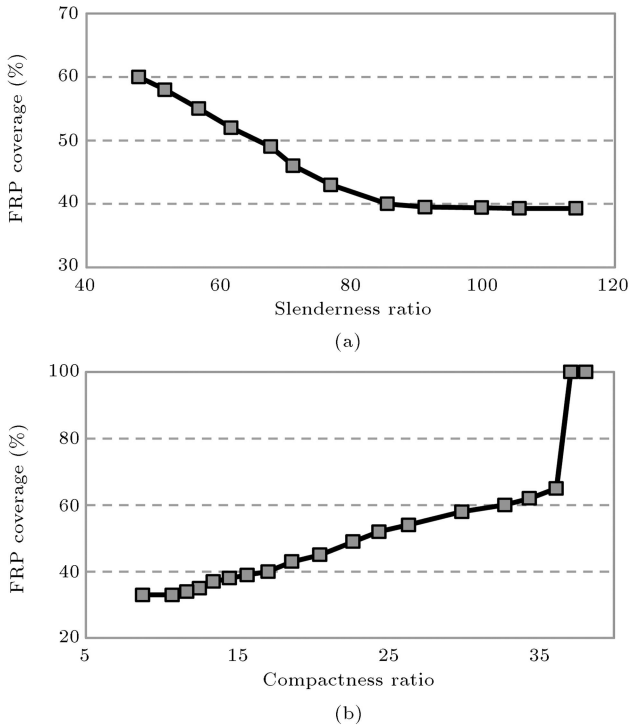

Figure 18. Effect of slenderness and compactness ratio on optimized length of FRP coverage: (a) Optimized FRP coverage length against slenderness ratio ($b/t = 22.6$) and (b) optimized FRP coverage length against compactness ratio ($kL/r = 67.9$).

it was assumed that the entire length of braces was strengthened.

5.2.1. Short braces

Figure 19(a) shows the axial load-axial displacement relationship for a short brace with various CFRP layers. According to this figure, adding the first layer of CFRP caused the most gain in enhancing the local buckling. When the number of CFRP layers increased to 3 layers, the buckling load increased. However, after employing the fourth layer, the compactness was sufficient enough for shifting the local buckling incident to the global buckling mode. Consequently, wrapping more FRP layers led to placing the border between short and intermediate brace domains, as depicted in Figure 8.

5.2.2. Intermediate braces

According to the classification defined earlier, strengthening the intermediate brace with 2 layers of CFRP changed its buckling mode from local to global buckling mode. According to Figure 19(b), when only one layer of CFRP was utilized, the transmission from local to global buckling did not take place. However, by adding more FRP layers, the dominant mode was converted from local to global buckling.

5.2.3. Long braces

Strengthening of long braces with one to four FRP

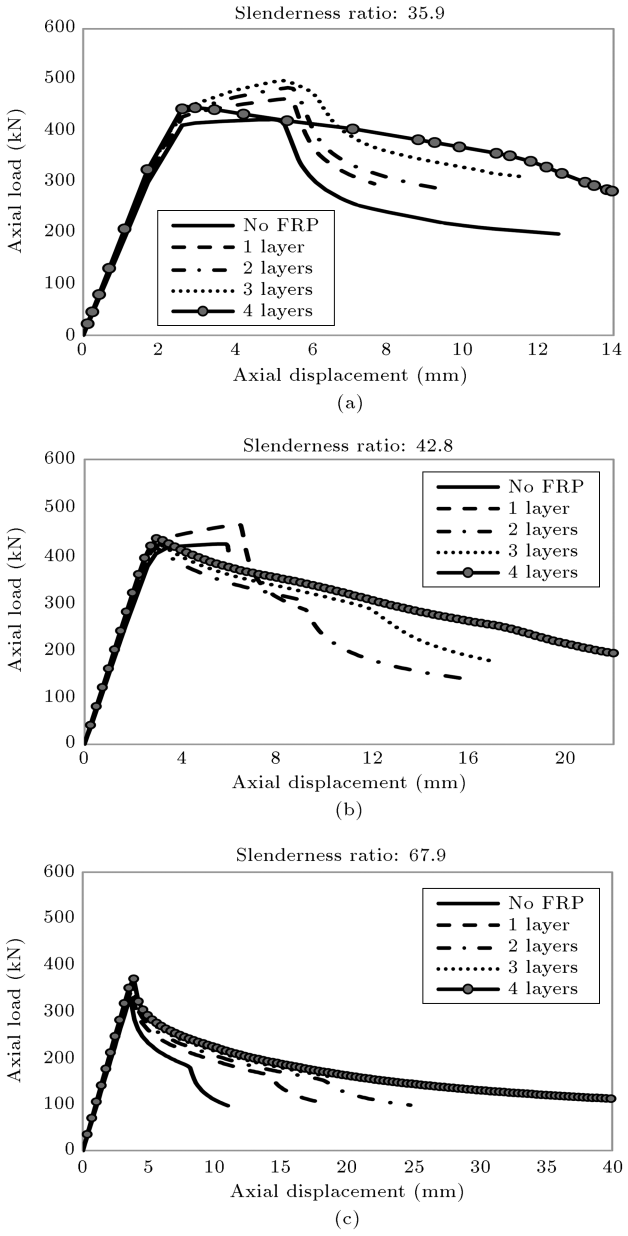

Figure 19. Axial load-axial displacement relationship for the short brace with different numbers of FRP layers: (a) Short brace, (b) intermediate brace, and (c) long brace.

layers was investigated for a typical SHS long brace with a slenderness ratio of 67.9. As can be seen in Figure 19(c), inserting the third layer of FRP has a significant role in delaying the local buckling mode. However, adding the fourth layer enhanced the performance of brace against local buckling, insignificantly. Moreover, for all models, no obvious rise in the value of peak strength was observed.

6. Conclusion

Diagonal Braces under earthquake load are expected to dissipate energy by buckling in compression and

yielding in tension [43]. The local buckling occurring after the overall buckling subjects the brace to the danger of fracture. According to previous studies, overwrapping transverse FRP sheets around a section is capable of preventing local buckling occurrence. Then, in this study, the use of FRP wrapping in the transverse direction was proposed. Such an FRP application seems to have the potential for suspending local buckling without resisting against the overall buckling, while the overall buckling of braces has a vital contribution to dissipating ground motion energy.

Consequently, a numerical model verified by previous research was developed to investigate the effect of FRP wrapping on the buckling behavior of braces. FRP sheets were considered to be transversely wrapped around the section, and key parameters including slenderness ratio, FRP length, and FRP coverage length, which can affect the strengthened brace performance, were investigated here. Moreover, the effect of slenderness and compactness ratios on FRP coverage length of long braces was studied specifically. The following results were drawn from the numerical study:

- An increase in strength attained by strengthening was the same for all short braces with different slenderness ratios as their performance was independent of slenderness ratio. However, for long braces, strengthening effect decreased with an increase in the slenderness ratio;
- Three types of behavior were observed by changing the slenderness ratio of strengthened braces. For the lower slenderness ratios, brace strengthening just increased the local buckling load. For braces with an intermediate slenderness ratio, strengthening could change the mode of failure from local to overall buckling. Finally, for greater slenderness ratios, strengthening just mitigated local buckling of the braces as the second mode of failure;
- FRP strengthening is able to make a considerable rise in seismic demands. Investigating the cyclic behavior of a wide range of braces demonstrated that FRP enhancement could postpone local buckling and subsequent fracture to the next cycles. Moreover, following strengthening, a significant increase was seen in ductility and energy dissipation;
- Adding more layers of FRP improved the effectiveness of strengthening in all braces. Furthermore, strengthening with FRP can reduce the boundary of the slenderness ratio between short and intermediate braces. For a short brace with a slenderness ratio of 35.9, using 4 layers of FRP can change the mode of buckling from local to overall. The same result was obtained for a longer brace with a slenderness ratio of 42.8 by applying two layers of CFRP;
- Partial strengthening of the short and intermediate braces cannot avoid the local buckling occurrence in the unstrengthened region. Conversely, for a long brace, by dominating overall buckling mode, degrading the FRP coverage up to the optimized length has no considerable effect on the quality of local buckling inhibition. However, employing FRP coverage of less than optimized length is incapable of preventing local buckling that occurred outside of the strengthening domain;
- With an appropriate parametric study for a long brace, it is possible to reduce FRP consumption and use an optimized length of coverage instead. The results of the study on the partial strengthening of long braces revealed that the optimized length of FRP coverage for local buckling mitigation was reduced for braces with larger slenderness ratios. Likewise, utilizing more compact sections decreased the minimum required length of FRP coverage, which is able to inhibit local buckling occurrence;
- Further study is still required to find other aspects of SHS brace strengthening.

Acknowledgement

We would like to express our gratitude to Dr. Heidarpour from Monash University for his invaluable comments that helped improve the current manuscript.

References

1. Gugerli, H. "Inelastic cyclic behavior of steel bracing members", Ph.D. Dissertation, Michigan University (1982).
2. Fell, B.V., *Large-Scale Testing and Simulation of Earthquake-Induced Ultra Low Cycle Fatigue in Bracing Members Subjected to Cyclic Inelastic Buckling*, University of California Davis (2008).
3. Sheehan, T., Chan, T.-M., and Lam, D. "Mid-length lateral deflection of cyclically-loaded braces", *Steel and Composite Structures*, **18**(6), pp. 1563-1576 (2015).
4. Shaback, B. and Brown, T. "Behaviour of square hollow structural steel braces with end connections under reversed cyclic axial loading", *Canadian Journal of Civil Engineering*, **30**(4), pp. 745-753 (2003).
5. Tremblay, R., Archambault, M.-H., and Filiatrault, A. "Seismic response of concentrically braced steel frames made with rectangular hollow bracing members", *Journal of Structural Engineering*, **129**(12), pp. 1626-1636 (2003).
6. American Institute of Steel Construction "AISC 341-05: Seismic provisions for structural steel buildings", American Institute of Steel Construction Inc, Chicago, IL (2005).
7. American Institute of Steel Construction "AISC 341-10: Seismic provisions for structural steel buildings",

American Institute of Steel Construction Inc, Chicago, IL (2010).

8. Nassirnia, M., Heidarpour, A., Zhao, X.-L., and Minkkinen, J. "Innovative hollow corrugated columns: A fundamental study", *Engineering Structures*, **94**, pp. 43-53 (2015).

9. Javidan, F., Heidarpour, A., Zhao, X.-L., and Minkkinen, J. "Performance of innovative fabricated long hollow columns under axial compression", *Journal of Constructional Steel Research*, **106**, pp. 99-109(2015).

10. Teng, J.G., Chen, J.F., Smith, S.T., Lam, L. *FRP Strengthened RC Structures*, UK: John Wiley & Sons (2002).

11. Bank, L.C., *Composites for Construction: Structural Design with FRP Materials*, John Wiley & Sons (2006).

12. Bakis, C., Bank, L.C., Brown, V., Cosenza, E., Davalos, J., Lesko, J., Machida, A., Rizkalla, S., and Triantafillou, T. "Fiber-reinforced polymer composites for construction-state-of-the-art review", *Journal of Composites for Construction* , **6**(2), pp. 73-87 (2002).

13. Teng, J., Yu, T., and Fernando, D. "Strengthening of steel structures with fiber-reinforced polymer composites", *Journal of Constructional Steel Research*, **78**, pp. 131-143 (2012).

14. Zhao, X.-L. and Zhang, L. "State-of-the-art review on FRP strengthened steel structures", *Engineering Structures*, **29**(8), pp. 1808-1823 (2007).

15. Mertz, D.R. and Gillespie Jr, J.W. "Rehabilitation of steel bridge girders through the application of advanced composite materials", (No. NCHRP-IDEA Project 011)" (1996).

16. Miller, T.C., Chajes, M.J., Mertz, D.R., and Hastings, J.N. "Strengthening of a steel bridge girder using CFRP plates", *Journal of Bridge Engineering*, **6**(6), pp. 514-522 (2001).

17. Tavakkolizadeh, M. and Saadatmanesh, H. "Fatigue strength of steel girders strengthened with carbon fiber reinforced polymer patch", *Journal of Structural Engineering*, **129**(2), pp. 186-196 (2003).

18. Ekiz, E., El-Tawil, S., Parra-Montesinos, G., and Goel, S. "Enhancing plastic hinge behavior in steel flexural members using CFRP wraps", *Proc., 13th World Conf. on Earthquake Engineering*, Vancouver (2004).

19. El-Tawil, S., Ekiz, E., Goel, S., and Chao, S.-H. "Retraining local and global buckling behavior of steel plastic hinges using CFRP", *Journal of Constructional Steel Research*, **67**(3), pp. 261-269 (2011).

20. Teng, J. and Hu, Y. "Behaviour of FRP-jacketed circular steel tubes and cylindrical shells under axial compression", *Construction and Building Materials*, **21**(4), pp. 827-838 (2007).

21. Sayed-Ahmed, E. "Strengthening of thin-walled steel I-section beams using CFRP strips", *Proceedings of the 4th Advanced Composites for Bridges and Structures Conference* (2004).

22. Eksi, S., Kapti, A.O., and Genel, K. "Buckling behavior of fiber reinforced plastic-metal hybrid-composite beam", *Materials & Design*, **49**, pp. 130-138 (2013).

23. Ragheb, W.F. "Inelastic local buckling and rotation capacity of steel I-beams strengthened with bonded FRP sheets", *Journal of Composites for Construction*, **21**(1), p. 04016058 (2017).

24. Shaat, A.A.S. "Structural behaviour of steel columns and steel-concrete composite girders retrofitted using CFRP", Ph.D. Dissertation, Queen's University (2007).

25. Shaat, A. and Fam, A.Z. "Slender steel columns strengthened using high-modulus CFRP plates for buckling control", *Journal of Composites for Construction*, **13**(1), pp. 2-12 (2009).

26. Shaat, A. and Fam, A. "Axial loading tests on short and long hollow structural steel columns retrofitted using carbon fibre reinforced polymers", *Canadian Journal of Civil Engineering*, **33**(4), pp. 458-470 (2006).

27. Bambach, M., Jama, H., and Elchalakani, M. "Axial capacity and design of thin-walled steel SHS strengthened with CFRP", *Thin-Walled Structures*, **47**(10), pp. 1112-1121 (2009).

28. Haedir, J. and Zhao, X.-L. "Design of short CFRP-reinforced steel tubular columns", *Journal of Constructional Steel Research*, **67**(3), pp. 497-509 (2011).

29. Park, J.-W. and Yoo, J.-H. "Axial loading tests and load capacity prediction of slender SHS stub columns strengthened with carbon fiber reinforced polymers", *Steel and Composite Structures*, **15**(2), pp. 131-150 (2013).

30. Feng, P., Hu, L., Qian, P., and Ye, L. "Buckling behavior of CFRP-aluminum alloy hybrid tubes in axial compression", *Engineering Structures*, **132**(Supplement C) pp. 624-636 (2017).

31. Kabir, M.Z. and Nazari, A.R. "Numerical study on reinforcing of thin walled cracked metal cylindrical columns using FRP patch", *Scientia Iranica transaction A-Civil Engineering*, **17**(5), pp. 407-414 (2010).

32. Teng, J. and Hu, Y. "Suppression of local buckling in steel tubes by FRP jacketing", *Proceedings, 2nd International Conference on FRP Composites in Civil Engineering*, Adelaide, Australia, pp. 8-10 (2004).

33. Batikha, M., Chen, J., Rotter, J., and Teng, J. "Strengthening metallic cylindrical shells against elephant's foot buckling with FRP", *Thin-Walled Structures*, **47**(10), pp. 1078-1091 (2009).

34. Haedir, J., Bambach, M., Zhao, X.-L., and Grzebieta, R. "Strength of circular hollow sections (CHS) tubular beams externally reinforced by carbon FRP sheets in pure bending", *Thin-Walled Structures*, **47**(10), pp. 1136-1147 (2009).

35. Zhao, X.-L., Fernando, D., and Al-Mahaidi, R. "CFRP strengthened RHS subjected to transverse end bearing force", *Engineering Structures*, **28**(11), pp. 1555-1565 (2006).

36. Alam, M.I., Fawzia, S., Zhao, X.-L., and Remennikov, A.M. "Experimental study on FRP-strengthened steel tubular members under lateral impact", *Journal of Composites for Construction*, **21**(5), p. 04017022 (2017).

37. Qingli, W. and Yongbo, S. "Compressive performances of concrete filled square CFRP-steel tubes (S-CFRP-CFST)", *Steel & Composite Structures: An International Journal*, **16**(5), pp. 455-480 (2014).

38. Yu, T., Hu, Y.M., and Teng, J.G. "Cyclic lateral response of FRP-confined circular concrete-filled steel tubular columns", *Journal of Constructional Steel Research*, **124**(Supplement C), pp. 12-22 (2016).

39. Harries, K.A., Peck, A.J., and Abraham, E.J. "Enhancing stability of structural steel sections using FRP", *Thin-Walled Structures*, **47**(10), pp. 1092-1101 (2009).

40. Kim, Y.J. and Harries, K.A. "Behavior of tee-section bracing members retrofitted with CFRP strips subjected to axial compression", *Composites Part B: Engineering*, **42**(4), pp. 789-800 (2011).

41. Gao, X., Balendra, T., and Koh, C. "Buckling strength of slender circular tubular steel braces strengthened by CFRP", *Engineering Structures*, **46**, pp. 547-556 (2013).

42. El-Tawil, S. and Ekiz, E. "Inhibiting steel brace buckling using carbon fiber-reinforced polymers: Large-scale tests", *Journal of Structural Engineering* , **135**(5), pp. 530-538 (2009).

43. Bruneau, M., Uang, C.-M., and Sabelli, S.R., *Ductile Design of Steel Structures*, McGraw Hill Professional (2011).

44. Davison, T. and Birkemoe, P. "Column behaviour of cold-formed hollow structural steel shapes", *Canadian Journal of Civil Engineering*, **10**(1), pp. 125-141 (1983).

45. Chan, S.L., Kitipornchai, S., and Al-Bermani, F.G. "Elasto-plastic analysis of box-beam-columns including local buckling effects", *Journal of Structural Engineering*, **117**(7), pp. 1946-1962 (1991).

46. ABAQUS/Standard, User's Manual- Version 6.11 (2011).

47. Hashin, Z. "Failure criteria for unidirectional fiber composites", *Journal of Applied Mechanics*, **47**(2), pp. 329-334 (1980).

48. Al-Zubaidy, H., Al-Mahaidi, R., and Zhao, X.-L. "Finite element modelling of CFRP/steel double strap joints subjected to dynamic tensile loadings", *Composite Structures*, **99**, pp. 48-61 (2013).

49. Fernando, N.D., *Bond Behaviour and Debonding Failures in CFRP-Strengthened Steel Members*, The Hong Kong Polytechnic University (2010).

Biographies

Parisa Shadan received her BS degree in Civil Engineering from Khaje Nasir Toosi University of Technology, Tehran, Iran in 2007 and her MS degree in Structural Engineering from Amirkabir University of Technology, Tehran, Iran in 2011. She is currently pursuing her PhD degree at Amirkabir University of Technology, Tehran, Iran. Her research interests include structural strengthening, seismic behavior of structures, fracture mechanics, composite materials, and finite element analysis.

Mohammad Zaman Kabir is a Professor at the Department of Civil and Environmental Engineering, Amirkabir University of Technology, Tehran, Iran. He received his BS and MS from Amirkabir University of Technology and PhD from Waterloo University in Canada. His research interest includes structural stability, structural analysis using FEM, experimental methods in structural engineering, composite structures, structural optimization, damage detection, and rehabilitation of structures.